Available online at www.sciencedirect.com

ScienceDirect

journal homepage: www.elsevier.com/locate/he

Co–Ce–Al–O mesoporous catalysts for hydrogen generation via ammonia decomposition

Hesam Maleki, Volfango Bertola *

Laboratory of Technical Physics, University of Liverpool, UK, Liverpool

HIGHLIGHTS

- The Co–Ce–Al–O mesoporous catalyst is prepared using a self-assembly method for ammonia decomposition.
- Ammonia conversion of 98% was obtained at 550 °C with the GHSV of 12,000 mL h^{-1} g_{cat}^{-1}.
- Cerium promoted the catalyst activity, and aluminium enhanced the catalyst stability.
- The Co–Ce–Al–O catalytic performance is comparable to Ru-based catalysts.

GRAPHICAL ABSTRACT

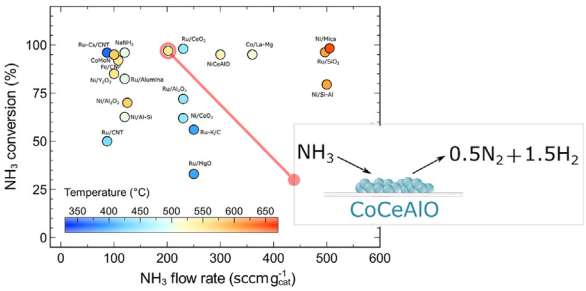

ARTICLE INFO

Article history:
Received 15 December 2021
Received in revised form
5 May 2022
Accepted 3 June 2022
Available online xxx

Keywords:
NH_3 decomposition
H_2 production
Cobalt-based catalysts
Mesoporous
Self-assembly

ABSTRACT

A series of Co–Ce–Al–O mesoporous catalysts synthesised by self-assembly is shown to be efficient for the hydrogen production via ammonia decomposition reaction. The evaporation-induced self-assembly method is utilised to effectively synthesise mesoporous multicomponent catalysts with tuned composition and improved performance. The prepared catalyst materials were characterised by several techniques including X-ray diffraction, scanning electron microscope, transmission electron microscope and N_2 physisorption analysis. The kinetic performance of the solid catalysts was evaluated at different temperatures and flow rates under atmospheric pressure. The optimised $Co_{0.5}Ce_{0.1}Al_{0.4}O$(sa) catalyst remained highly active below 550 °C which represents a competitive performance among state-of-the-art catalysts. The promising performance of the catalyst and the use of nonprecious metals in the structure represent a feasible approach towards the application of ammonia as a hydrogen carrier for on-board hydrogen production.

* *Corresponding author.*
E-mail address: Volfango.Bertola@liverpool.ac.uk (V. Bertola).

https://doi.org/10.1016/j.ijhydene.2022.06.021

Introduction

Hydrogen is one of the most promising green fuels, however, has limitations in delivery and storage due to the low volumetric density and high flammability [1]. Among the various hydrogen delivery technologies, hydrogen generation from ammonia decomposition has been actively pursued recently [2,3]. Ammonia releases 17.8 wt% of hydrogen through a CO_x−free reaction process: $NH_3(g) \rightarrow 0.5N_2(g) + 1.5H_2(g)$ [3]. Ammonia can be compressed in liquid form under mild conditions (room temperature and 10 bar) in which contains higher volumetric H_2 density than that of liquid hydrogen [4,5]. Furthermore, ammonia has well-established production and transportation infrastructure compared to recent H_2 carrier alternatives [6].

Because of the kinetic limitations of the ammonia decomposition reaction and its endothermic nature, a high operating temperature (up to 800 °C) is required to perform the ammonia decomposition at high conversions through a catalytic reaction. For this reason, many studies have been conducted about new catalyst designs for ammonia decomposition to enhance the activity at lower reaction temperatures [2]. There is a consensus on ruthenium as the most active element for the ammonia decomposition reaction [7,8]. Ganley et al. investigated various metals doped on Al_2O_3 support and reported the catalyst activity order as: Ru > Ni > Rh > Co > Ir > Fe > Pt > Cr > Pd > Cu [9]. Many studies are available in the literature for the ammonia decomposition reaction on noble metals (*e.g.*, Ru, Rh, Ir) [10,11], transition metals (*e.g.*, Ni, Fe, Mo, Co) [12–14], and more recently, on metal amides/imides [15,16] and multicomponent composite catalysts [14,17,18].

Because of the high cost and the scarcity of precious metals, multicomponent transitional metal catalysts have been widely studied as low-cost efficient alternatives. Gu et al. [19] studied the performance of Fe, Co and Ni nanoparticles dispersed in alumina support for the ammonia decomposition reaction and the Co/Al catalyst showed the highest activity among others. Lucentini et al. [8] investigated the performance of ruthenium-based catalysts loaded on Al_2O_3 and CeO_2 supports. The Ru/CeO_2 was the most active catalyst but with limited durability due to the Ru volatilization. Among the typical promoters and supports for ammonia decomposition catalysts, cerium has been recently reported to show high performance. In addition, the presence of even a small amount of alumina in the catalyst structure is found to impede the agglomeration of active crystallites and enhance the catalyst stability during the reaction [19]. Therefore, based on these studies, Co–Ce–Al metallic structure could be a potential catalyst for the low-temperature ammonia decomposition.

Mesoporous metal oxide materials (MMOMs) have attracted increasing attention due to their unique properties and applications in the field of catalysis [20–22], electronics [23,24], drug delivery [25,26] and environmental science [27]. MMOMs possess high surface area, ordered unblocked pore structure, thermal stability and exceptional redox properties which make them well-suited for different applications, specifically as catalyst supports. Due to larger pore diameters and thermal stability, the reactant molecules can interact more effectively with the active sites on the large internal surfaces of the mesoporous catalyst at elevated temperatures [28,29]. Various methods are used to synthesise mesoporous metal oxide materials such as sol-gel chemistry, impregnation and coprecipitation methods. These techniques are mostly complex, time-consuming or incapable of mass production. Furthermore, some of their synthesised products suffer from low stability, poor activity and sintering of active sites at high temperatures [29,30]. In recent years, a self-assembly approach has been introduced for continuous, fast production of mesoporous nanoparticles. The evaporation-induced self-assembly approach (EISA) uses the block copolymer as a soft template which is removed after the evaporation-induced self-assembly. The EISA approach has been adapted and utilised to produce MMOMs with high surface area [31,32].

Huang et al. [30] prepared the $Ce_{0.6}Zr_{0.3}Y_{0.1}O_2$ support by a soft-template self-assembly method and Ni, Co and Ni–Co components were doped by incipient wet-impregnation. The synthesised catalysts showed high activity and stability, and the ammonia conversion approached 100% at 600 °C with the GHSV (gas hourly space velocity) of 6000 mL h^{-1} g_{cat}^{-1}. Yan et al. [29] used the aerosol-assisted self-assembly approach (AASA) to synthesise mesoporous multimetal oxide microspheres (Ni–Ce–Al–O) from metal nitrates. The tricomponent Ni–Ce–Al–O composite catalysts exhibited higher activity and durability over NiO or bimetallic catalysts (Ni–Ce–O and Ni–Al–O).

Following the recent reports, the present work is aimed at developing a low-cost highly active class of catalysts for the H_2 production from the NH_3 decomposition reaction. Here, the evaporation-induced self-assembly method is demonstrated for the synthesis of a series of mesoporous metal oxides (Co–Ce–Al–O) from metal nitrates. The synthesised catalysts are comprehensively characterised and later tested for the NH_3 decomposition under different reaction conditions. The reaction kinetics is examined in a tubular reactor, as well as the catalyst durability under a long-term reaction run.

Experimental

Catalyst preparation

The Co–Ce–Al–O mesoporous materials were prepared using a self-assembly method. 0.5 g of triblock copolymer F-127 Pluronic (Sigma-Aldrich) was added into 50 mL of ethanol as a soft template. Certain molar ratios of metal salts including $Co(NO_3)_2 \cdot 6H_2O$ (99%, ACROS Organics™), $Ce(NO_3)_3 \cdot 6H_2O$ (99%, Sigma-Aldrich) and $Al(NO_3)_3 \cdot 9H_2O$ (99%, ACROS Organics™) with the overall amount of 5 mmol were dissolved in the solution. The final solution was stirred for 1 h and placed into an oven for 3 days at 70 °C. The samples were dried and polymerised into metal oxide network at this stage. Later on, the sample gels were calcined in air at 500 °C for 4 h with a heating rate of 1 °C/min, and the ultimate catalyst powders were obtained. During calcination, the catalyst samples were crystallized, and Pluronic F-127 was completely removed leading to the formation of mesoporous structures. The synthesised catalysts were labelled as $Co_xCe_yAl_zO$(sa) where 'sa' referred to the self-assembly method, and the 'xyz' subscripts were assigned to the molar ratios of metal elements, x:y:z ≡

Please cite this article as: Maleki H, Bertola V, Co–Ce–Al–O mesoporous catalysts for hydrogen generation via ammonia decomposition, International Journal of Hydrogen Energy, https://doi.org/10.1016/j.ijhydene.2022.06.021

0.9:0.0:0.1, 0.5:0.4:0.1, 0.5:0.1:0.4, 0.8:0.1:0.1. A series of catalysts with the same composition was synthesised using a simple coprecipitation (cp) method [33] and calcined at 500 °C for 4 h for comparison.

Catalyst characterisation

The crystallite phases of the catalyst samples were characterised with X-ray diffraction (XRD) using a Rigaku MiniFlex 600 diffractometer operating with Cu Kα radiation at 30 kV and 15 mA. Diffraction data (2θ) were collected between 20° and 70° with a step interval of 0.1°. Crystallography Open Database (COD) was used as the reference for the phase analysis of catalyst materials. A JEOL JSM-7001F scanning electron microscope operated at 5 kV was selected to produce the SEM images as well as the energy-dispersive X-ray spectroscopy (EDX) results. Dried catalyst powders were simply immobilized onto carbon adhesive discs for SEM analysis. To obtain higher resolution micrographs, a JEM-2100 transmission electron microscope (TEM) was used equipped with a lanthanum hexaboride (LaB_6) filament operating at 200 kV. The surface area of the catalyst samples was measured at 77 K from N_2 adsorption-desorption by means of a Micromeritics 3-FLEX instrument. The samples were outgassed under vacuum at 300 °C for 3 h to remove moisture or other adsorbed gases from the sample surface. The BET method was selected to obtain the specific surface area and pore size distribution.

Catalytic experiments

For the catalyst performance analysis, a tubular reactor (stainless steel tube, inner diameter: 6 mm) was used, and pure anhydrous ammonia gas was passed over the catalyst powder (≈0.5 g) inside the reactor. The catalytic studies were performed on $Co_xCe_yAl_zO$ mesoporous samples prepared using both methods (self-assembly and coprecipitation). 0.5 wt%Ru/Al_2O_3 pellets (3.2 mm, Sigma-Aldrich) were purchased and tested as the reference catalyst. The schematic layout of the ammonia decomposition set-up is given in Fig. 1. The set-up comprises an NH_3 cylinder, flow meters, fittings, valves, a tubular furnace (heater), NH_3 absorbers, and the cracking reactor. The ammonia cylinder (Ammonia Micrographic Grade, BOC) had a pressure controller in stainless steel for use with corrosive anhydrous ammonia. Two variable-area flow meters were installed to measure the flow rate of NH_3 at the inlet and the NH_3–free cracking product (N_2 and H_2) at the set-up outlet, respectively. Gas flow rates were recorded in standard cubic centimetres per minute (sccm). Moreover, the ammonia conversions were calculated based on volumetric flowmetry. The ammonia residue was removed from the reaction product using two ammonia absorbers containing hydrogen chloride solution prior to the outlet flow measurements. The NH_3 conversions were then measured assuming that the gas product is made up of only hydrogen and nitrogen gas using the following equation [3,14]:

$$NH_3\text{Conversion}\,(\%) = 100 \times \frac{F_{out}}{2F_{in}}, \quad (1)$$

where F_{in} and F_{out} are the flow rates of inlet NH_3 feed and outlet flow (NH_3-free), respectively.

To study the process temperature, ammonia conversions were measured within the reaction temperature range of 350–650 °C at different temperature intervals. The blank tubular reactor was also examined to observe the ammonia conversions through the catalyst-free process and measuring the volume-based homogenous reaction. The conversion data were recorded after 1 h of reaction run to reach the steady-state condition. The catalyst sample also goes through self-activation (under ammonia flow) at this step. The ammonia feed flow rate was set to 50–500 sccm for catalytic activity measurements. The catalyst stability tests were performed under 200 sccm g_{cat}^{-1} ammonia flow at 500 °C and 550 °C for 48 h, and the ammonia conversions were recorded continuously. The apparent activation energies for the ammonia decomposition reaction were obtained at low conversions ($X_{NH_3} = 10 - 13\%$) at 350–450 °C.

Results and discussion

Characterisation

X-ray diffraction analysis

Fig. 2 displays the X-ray diffraction peaks corresponding to the cubic cobalt oxide (Co_3O_4) and cubic cerianite (CeO_2)

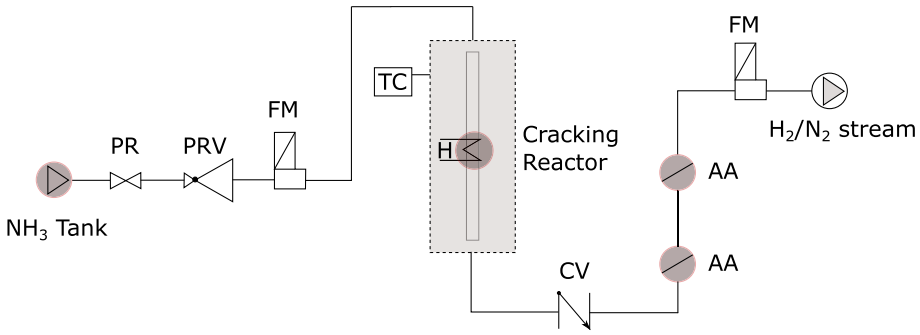

Fig. 1 – Layout of the ammonia decomposition set-up using the tubular reactor; PR: pressure regulator, PRV: pressure reducing valve, FM: flow meter, CV: check valve, TC: temperature controller, H: heater, AA: ammonia absorber. Reprinted with permission from Ref. [3].

Please cite this article as: Maleki H, Bertola V, Co–Ce–Al–O mesoporous catalysts for hydrogen generation via ammonia decomposition, International Journal of Hydrogen Energy, https://doi.org/10.1016/j.ijhydene.2022.06.021

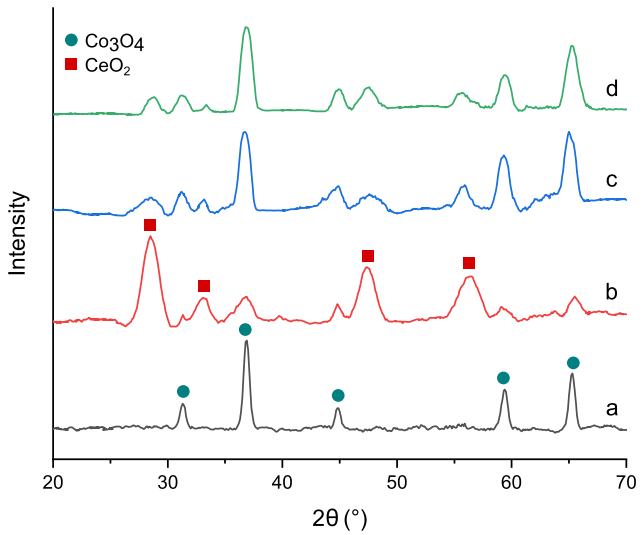

Fig. 2 – XRD diffraction patterns of catalyst samples: (a) $Co_{0.9}Al_{0.1}O$(sa), (b) $Co_{0.5}Ce_{0.4}Al_{0.1}O$(sa), (c) $Co_{0.5}Ce_{0.1}Al_{0.4}O$(sa) and (d) $Co_{0.8}Ce_{0.1}Al_{0.1}O$(sa).

crystallized in the structure of the catalysts. There is no trace of crystalline Al_2O_3 phase in the XRD patterns which suggests its disordered nature as reported in the literature [29]. The crystalline properties of the examined mesoporous samples are summarised in Table 1. The particle domain size of cobalt oxide was measured to be 13.1, 8.5, 7.8, and 8.6 nm for $Co_{0.9}Al_{0.1}O$(sa), $Co_{0.5}Ce_{0.4}Al_{0.1}O$(sa), $Co_{0.5}Ce_{0.1}Al_{0.4}O$(sa) and $Co_{0.8}Ce_{0.1}Al_{0.1}O$(sa) catalysts, respectively, using the Scherrer equation. Hence, the domain size of cobalt oxide was decreased after the addition of alumina and ceria components into the catalyst structure, leading to the better dispersion of cobalt.

Electron microscopy

The catalyst morphology was studied by scanning electron microscopy (SEM). The representative SEM images of $Co_xCe_yAl_zO$(sa) samples prepared by soft-template self-assembly method are shown in Fig. 3.

Two distinctive structures were observed in the prepared samples: i) relatively large porous grains of irregular shape with the rather smooth external surface having sub-100 nm features in $Co_{0.9}Al_{0.1}O$(sa) and $Co_{0.5}Ce_{0.1}Al_{0.4}O$(sa) (a, c) samples; ii) sponge-like morphology with rounded particles with an average size ranging from 100 to 300 nm in $Co_{0.5}Ce_{0.4}Al_{0.1}O$(sa) and $Co_{0.8}Ce_{0.1}Al_{0.1}O$(sa) (b, d) samples. Furthermore, the latter structure did not appear in the case of the catalysts synthesised by standard coprecipitation (Fig. S2). It is concluded that this unique structure is a result of the decomposition of the copolymer's network, after the calcination process.

Elemental mapping was conducted with the energy dispersive X-Ray analysis (EDX) to visualize the Co–Ce–Al distribution on the catalyst surface. The molar ratios of elements in the prepared samples were in agreement with the actual values measured by EDX elemental mapping (Table S2). Fig. 4 shows the homogeneous distribution of individual metals of $Co_{0.5}Ce_{0.1}Al_{0.4}O$(sa) catalyst. This confirms that the uniformity of Co, Ce and Al is extended all over the catalyst structure.

The TEM micrograph of the $Co_{0.5}Ce_{0.1}Al_{0.4}O$(sa) sample illustrates that the mesoporous structure of the catalyst is formed in the framework. The synthesised sample is comprised mainly of tiny uniform particles with the size ranging from ≈10 to 20 nm (Fig. 5).

N_2 physisorption analysis

Surface properties of the synthesised mesoporous catalysts are summarised in Table 1. Based on the BET analysis, the mesoporous synthesised $Co_{0.5}Ce_{0.1}Al_{0.4}O$(sa) sample showed the highest surface area. In addition, in the self-assembled samples, the large grain structure belongs to the samples with higher surface area: 159.5 and 22.2 $m^2\ g^{-1}$ for $Co_{0.5}Ce_{0.1}Al_{0.4}O$(sa) and $Co_{0.9}Al_{0.4}O$(sa), respectively. The sample with the highest surface area and pore volume contains the highest Al molar ratio (= 0.4) in its structure among others. This implies that Al in the catalyst structure enhances the catalyst surface area significantly. Furthermore, the pore size in all prepared catalysts lies within the range of 8–22 nm, which is the characteristic of mesoporous materials. Fig. 5b shows the nitrogen adsorption-desorption isotherm of $Co_{0.5}Ce_{0.1}Al_{0.4}O$(sa) catalyst sample. During the N_2 physisorption of mesoporous materials, a hysteresis loop appears in the adsorption-desorption isotherm due to the multilayer adsorption process followed by capillary condensation [34], which is noticeable in the sample nitrogen isotherm. All samples including $Co_{0.5}Ce_{0.1}Al_{0.4}O$(sa) show type IV with H3-type hysteresis loops based on the IUPAC classification, suggesting that the sample aggregates are plate-like particles forming slit-like pores with accessible connectivity [30] (Fig. S3).

Catalytic reaction study

In order to study the performance of synthesised mesoporous catalysts in the ammonia decomposition, the reaction kinetics

Table 1 – Physical properties of synthesised mesoporous catalysts.

Catalyst	XRD size[a] (nm)	BET surface area ($m^2\ g^{-1}$)	Pore volume ($cm^3\ g^{-1}$)	Pore diameter (nm)
$Co_{0.9}Al_{0.1}O$(sa)	13.1 [Co]	22.2	0.11	21.8
$Co_{0.5}Ce_{0.4}Al_{0.1}O$(sa)	8.5 [Co], 6.2 [Ce]	6.5	0.017	8.8
$Co_{0.5}Ce_{0.1}Al_{0.4}O$(sa)	7.8 [Co], 5.3 [Ce]	159.5	0.64	15
$Co_{0.8}Ce_{0.1}Al_{0.1}O$(sa)	8.6 [Co], 7.4 [Ce]	14.9	0.047	12.6
0.5 wt%Ru/Al_2O_3		127.5	0.3	8.2

[a] Measured from XRD profiles using the Scherrer equation.

Please cite this article as: Maleki H, Bertola V, Co–Ce–Al–O mesoporous catalysts for hydrogen generation via ammonia decomposition, International Journal of Hydrogen Energy, https://doi.org/10.1016/j.ijhydene.2022.06.021

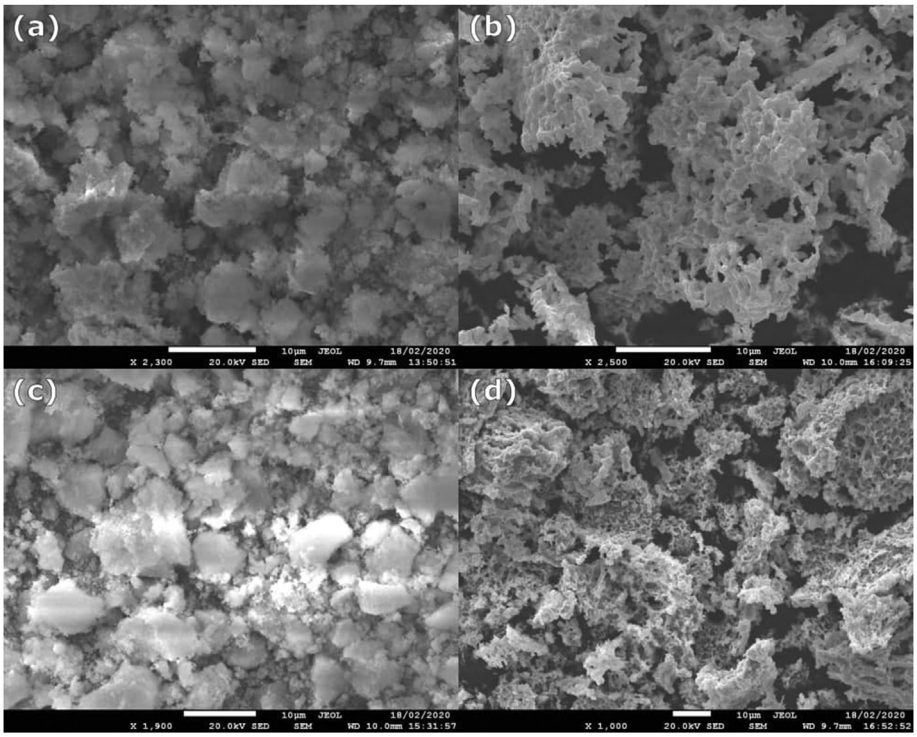

Fig. 3 – SEM images of mesoporous samples prepared by self-assembly method: (a) $Co_{0.9}Al_{0.1}O$(sa), (b) $Co_{0.5}Ce_{0.4}Al_{0.1}O$(sa), (c) $Co_{0.5}Ce_{0.1}Al_{0.4}O$(sa) and (d) $Co_{0.8}Ce_{0.1}Al_{0.1}O$(sa).

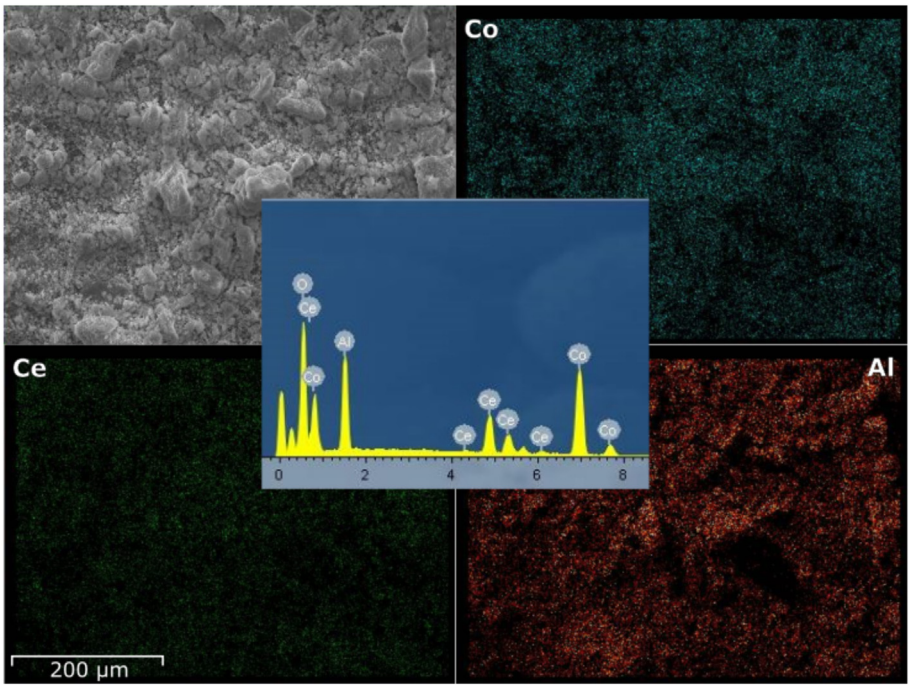

Fig. 4 – EDX elemental mapping of $Co_{0.5}Ce_{0.1}Al_{0.4}O$(sa) catalyst.

was studied in detail. $Co_xCe_yAl_zO$ mesoporous composites were examined as potential catalysts along with 0.5 wt%Ru/Al_2O_3 as reference. The kinetic tests were conducted at different reaction temperatures and NH_3 feed flow rates.

Effect of reaction temperature

The composition–activity relation of prepared catalysts for the NH_3 decomposition at an NH_3 flow rate of 100 sccm is compared and shown in Fig. 6. Ammonia conversion was

Please cite this article as: Maleki H, Bertola V, Co–Ce–Al–O mesoporous catalysts for hydrogen generation via ammonia decomposition, International Journal of Hydrogen Energy, https://doi.org/10.1016/j.ijhydene.2022.06.021

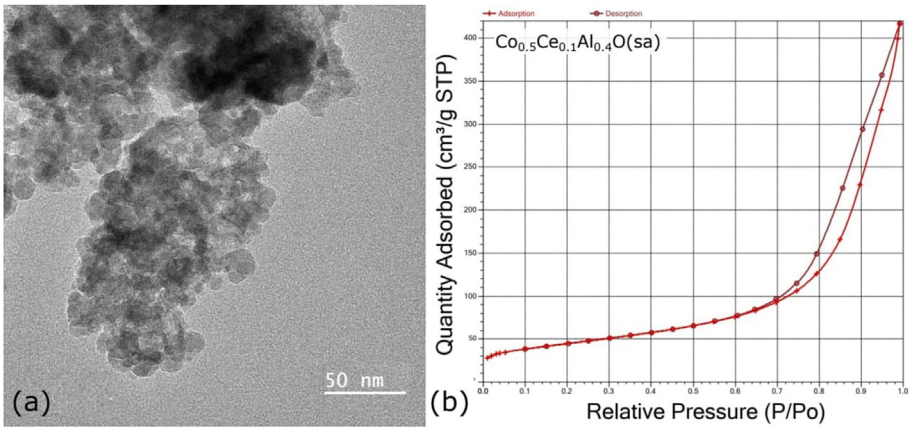

Fig. 5 – TEM image (a) and N_2 adsorption-desorption isotherm (b) for the synthesised $Co_{0.5}Ce_{0.1}Al_{0.4}O(sa)$ catalyst.

increased with the reaction temperature in the range of 350–600 °C. For all tested samples, the ammonia conversions were higher compared to that for the blank reactor, and the catalyst performance was noticeably improved after the addition of cerium species. The surface properties (*e.g.*, BET surface area) play key roles in the catalyst activity as well as the catalyst composition. The highest activity belongs to $Co_{0.5}Ce_{0.1}Al_{0.4}O(sa)$ sample prepared by self-assembly method. This catalyst sample has the highest surface area, pore volume and Al molar ratio (= 0.4) in its formulation. This suggests that Al component in the catalyst samples enhances the surface area resulting in higher activity. Therefore, $Co_{0.5}Ce_{0.1}Al_{0.4}O(sa)$ sample was selected as the optimised catalyst for later studies. The catalytic activity results of the coprecipitated catalyst samples are given in Fig. S5 and Fig. S6. Such differences in the NH_3 conversion of the samples with the same compositions may be related to the preparation procedure leading to different morphologies.

Effect of NH_3 flow rate

The kinetics of ammonia decomposition was further studied over the prepared catalysts (0.5 g) at 550 °C, undertaken at various flow rates: 50–500 sccm, in the tubular reactor. The recorded results for the catalyst samples are shown in Fig. 7.

The blank reactor converts about 3–10% of ammonia feed at 550 °C within the tested flow rate range due to the homogeneous volume-based reaction. All the prepared samples could achieve high NH_3 conversion efficiencies at lower flow rates (< 100 sccm). There is a rapid increase in conversions when the NH_3 flow rates fall below ≈250 sccm for the prepared MMOMs.

Higher NH_3 flow rates (up to 500 sccm) were also investigated to explore the H_2 generation capacity of the synthesised catalysts. Generally, the NH_3 conversion decreased with the flow rate elevation with a mild slope at higher flow rates (> 250 sccm). In spite of the mild decrease in NH_3 conversions, more H_2 volume can be produced at higher flow rates [15]. The hydrogen generation rate for two selected samples and in the blank reactor at 550 °C for different flow rates is shown in Fig. 8. The highest calculated H_2 generation rate was 397 sccm

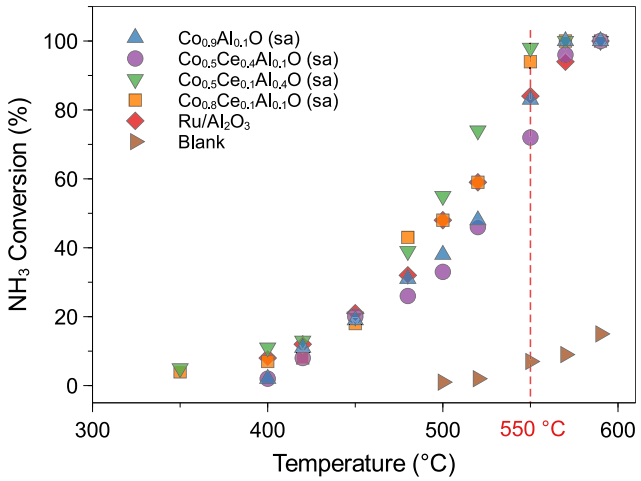

Fig. 6 – Comparison of NH_3 conversion as a function of reaction temperature (between 350 and 600 °C) for the blank tubular reactor (6 cm^3), 0.5 g of Ru/Al_2O_3 and $Co_xCe_yAl_zO(sa)$ catalysts prepared by self-assembly at an NH_3 flow rate of 100 sccm.

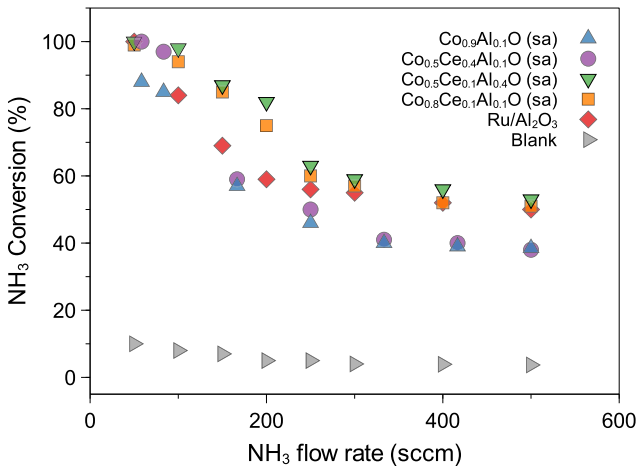

Fig. 7 – Conversions of NH_3 obtained at 50–500 sccm flow within a 6 cm^3 reactor for 0.5 g of Ru/Al_2O_3 and $Co_xCe_yAl_zO(sa)$ catalysts prepared by self-assembly at 550 °C.

Please cite this article as: Maleki H, Bertola V, Co–Ce–Al–O mesoporous catalysts for hydrogen generation via ammonia decomposition, International Journal of Hydrogen Energy, https://doi.org/10.1016/j.ijhydene.2022.06.021

for $Co_{0.5}Ce_{0.1}Al_{0.4}O$(sa) sample, equivalent to 53% conversion for 500 sccm ammonia feed.

The Co–Ce–Al–O mesoporous catalyst prepared in this work showed promising performance during the reaction runs, and it could be a potential alternative to the catalysts based on precious metals with respect to catalytic activity. A comparison of recent reports on newly synthesised catalysts for the low-temperature ammonia decomposition is summarised in Fig. 9. The ammonia conversion efficiencies are shown versus variable NH_3 flow rates at different recorded temperatures in the literature. The studied flow rates are reported based on catalyst content (sccm g_{cat}^{-1}) to allow for a comparative study. These reports are for pure NH_3 as the reaction feed except Lucentini et al. [8] and Bell et al. [18] where Ar/NH_3 and He/NH_3 mixtures were used, respectively. One may consider TOF values for a more sensible comparison. The optimised catalyst sample in this work is denoted with a red arrow in Fig. 9 (98%, 200 sccm g_{cat}^{-1}, 550 °C).

Blank reactor

The NH_3 conversion data were recorded for the blank tubular reactor (ca. 6 cm^3) for the 500–650 °C range at NH_3 flow rates of 50 and 100 sccm as shown in Fig. 10. The blank reactor alone produced an NH_3 conversion of 0–20% at temperatures lower than 600 °C. However, the NH_3 conversion efficiencies were increased more rapidly at higher temperatures and reached ≈ 60% at 650 °C.

The reaction rate in the blank reactor is due to the volumetric homogenous reaction in the absence of the heterogeneous catalyst. The reactor volume in the tubular reactor was designed small enough to neglect the effect of volumetric reaction rate at temperatures lower than 600 °C, to assure that the reaction rate mainly occurs on the surface of the loaded catalyst.

Activation energy measurements

The apparent activation energies (E_{app}) of ammonia decomposition reaction over the optimised sample and Ru/Al_2O_3 are shown in Fig. 11.

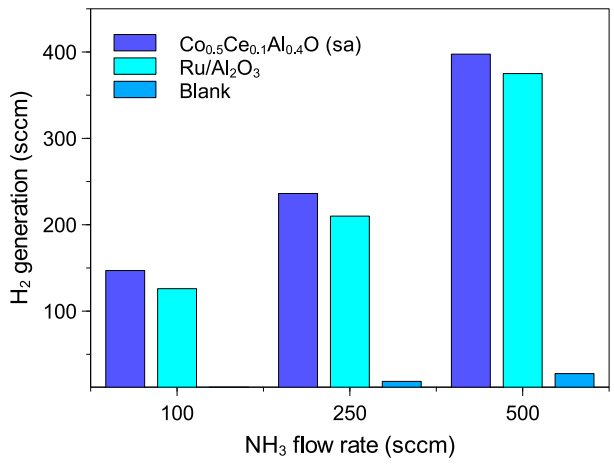

Fig. 8 – Hydrogen generation rate for 0.5 g of $Co_{0.5}Ce_{0.1}Al_{0.4}O$(sa) and Ru/Al_2O_3 catalysts and in the blank reactor at 550 °C for three NH_3 flow rates: 100, 250 and 500 sccm.

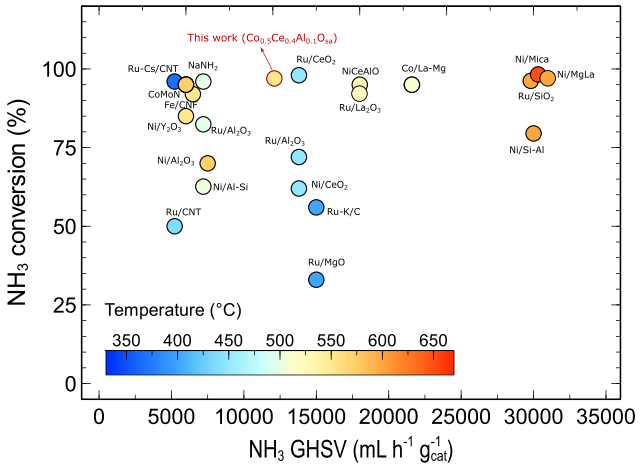

Fig. 9 – Recent reports on the activity of novel catalysts for the low-temperature ammonia decomposition reaction: Ru–Cs/CNT [35], CoMoN [14], $NaNH_2$ [15], Fe/CNF [12], Ni/Y_2O_3 [13], Ru/Alumina [15], Ni/Al_2O_3 [36], Ni/Al-Si [15], Ru/CNT [18], Ru/CeO_2 [8], Ru/Al_2O_3 [8], Ni/CeO_2 [8], Ru–K/C [37], Ru/MgO [37], NiCeAlO [18], Ru/La_2O_3 [38], Co/La-Mg [17], Ni/Mica [39], Ru/SiO_2 [11], Ni/MgLa [40], Ni/Si-Al [11].

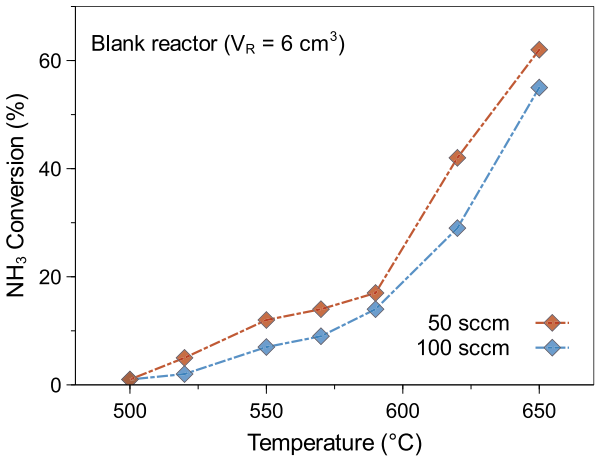

Fig. 10 – Comparison of NH_3 conversion as a function of reaction temperature for the blank 6 cm^3 tubular reactor at NH_3 flow rates of 50 and 100 sccm.

The E_{app} measurements indicated small differences between the activation energies of the tested catalyst samples. The difference in performance may originate from the different catalyst textural structures [29]. However, the activation energy of $Co_{0.5}Ce_{0.1}Al_{0.4}O$(sa) was marginally lower leading to a higher activity.

Catalyst durability test

Fig. 12 shows the durability of $Co_{0.5}Ce_{0.1}Al_{0.4}O$(sa) catalyst at two different temperatures for a 48 h reaction run. The ammonia decomposition was performed in a tubular reactor at temperature steps of 550 °C (for 25 h) and 500 °C (for 20 h) with an NH_3 flow rate of 200 sccm g_{cat}^{-1}. The catalyst sample showed great stability during the long-term tests. This could be attributed to the presence of Al and Ce species in the

Please cite this article as: Maleki H, Bertola V, Co–Ce–Al–O mesoporous catalysts for hydrogen generation via ammonia decomposition, International Journal of Hydrogen Energy, https://doi.org/10.1016/j.ijhydene.2022.06.021

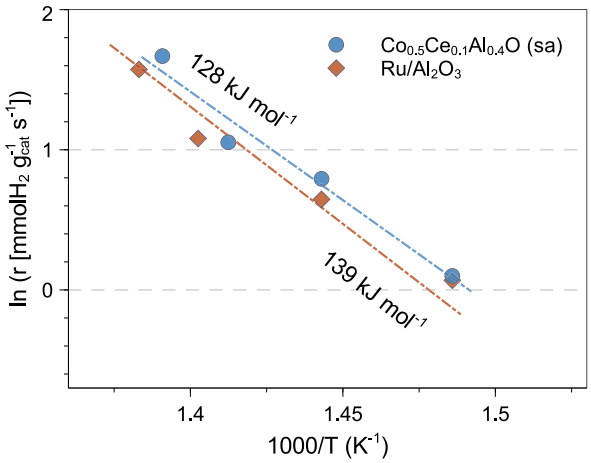

Fig. 11 – The Arrhenius plots and the corresponding activation energy (E_a) values for the NH_3 decomposition over $Co_{0.5}Ce_{0.1}Al_{0.4}O$(sa) and Ru/Al_2O_3. Adapted with permission from Ref. [3].

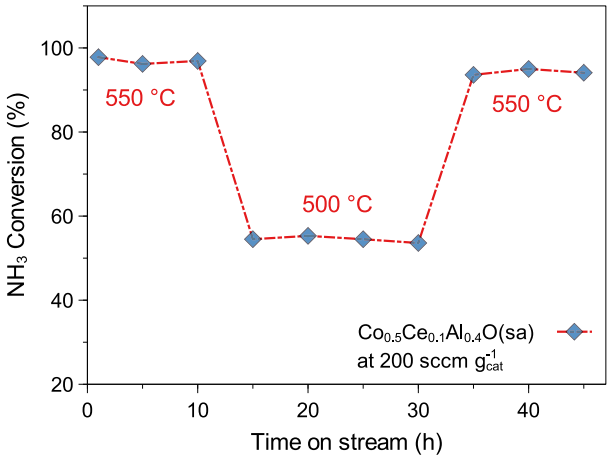

Fig. 12 – Stability test of $Co_{0.5}Ce_{0.1}Al_{0.4}O$(sa) catalyst (0.5 g) as a function of time at 500 and 550 °C reaction temperatures and 200 sccm g_{cat}^{-1} NH_3 flow rate (GHSV = 12,000 mL h^{-1} g_{cat}^{-1}).

catalyst structure. The addition of Al effectively suppressed the sintering of Co and Ce species and enhanced the catalyst thermal stability, active site distribution and catalyst surface area [29]. The presence of Ce in the catalyst structure assisted in catalyst durability as similarly reported by other authors [8,41].

Conclusions

A self-assembly approach was selected to synthesise mesoporous catalysts from non-noble metals for the hydrogen generation from ammonia decomposition reaction. The combination of characterisation techniques and kinetic studies on the Co–Ce–Al–O case study revealed the relationship between the catalyst physical and chemical properties and its performance. The presence of cerium promoted the catalyst activity, and doping aluminium into the catalyst structure enhanced the catalyst stability and active surface area. The self-assembled Co–Ce–Al–O catalyst with the Co:Ce:Al molar ratio of 0.5:0.1:0.4 showed the highest ammonia conversion of 98% at 550 °C with the GHSV of 12,000 mL h^{-1} g_{cat}^{-1}. Furthermore, the optimised catalyst exhibited high thermal stability during the 48 h reaction run.

Declaration of competing interest

The authors declare that they have no known competing financial interests or personal relationships that could have appeared to influence the work reported in this paper.

Acknowledgements

This work was supported by the European Regional Development Fund through Low Carbon Eco-Innovatory (LCEI) project Grant 22R15P00045, in partnership with CAL International Ltd. The TEM/SEM experiments in this paper were performed in the Albert Crewe Centre for Electron Microscopy at the University of Liverpool by Dr Mounib Bahri.

Appendix A. Supplementary data

Supplementary data to this article can be found online at https://doi.org/10.1016/j.ijhydene.2022.06.021.

REFERENCES

[1] Huang D-C, Jiang C-H, Liu F-J, Cheng Y-C, Chen Y-C, Hsueh K-L. Preparation of Ru–Cs catalyst and its application on hydrogen production by ammonia decomposition. Int J Hydrogen Energy 2013;38(8):3233–40. https://doi.org/10.1016/j.ijhydene.2012.10.105.
[2] Mukherjee S, Devaguptapu SV, Sviripa A, Lund CRF, Wu G. Low-temperature ammonia decomposition catalysts for hydrogen generation. Appl Catal, B 2018;226:162–81.
[3] Maleki H, Fulton M, Bertola V. Kinetic assessment of H_2 production from NH_3 decomposition over CoCeAlO catalyst in a microreactor: experiments and CFD modelling. Chem Eng J 2021;411:128595.
[4] Klerke A, Christensen CH, Nørskov JK, Vegge T. Ammonia for hydrogen storage: challenges and opportunities. J Mater Chem 2008;18(20):2304–10.
[5] Akiyama M, Aihara K, Sawaguchi T, Matsukata M, Iwamoto M. Ammonia decomposition to clean hydrogen using non-thermal atmospheric-pressure plasma. Int J Hydrogen Energy 2018;43(31):14493–7. https://doi.org/10.1016/j.ijhydene.2018.06.022.
[6] Lan R, Irvine JTS, Tao S. Ammonia and related chemicals as potential indirect hydrogen storage materials. Int J Hydrogen Energy 2012;37(2):1482–94.
[7] Yin SF, Xu BQ, Zhou XP, Au CT. A mini-review on ammonia decomposition catalysts for on-site generation of hydrogen for fuel cell applications. Appl Catal, A 2004;277(1):1–9.

[8] Lucentini I, Casanovas A, Llorca J. Catalytic ammonia decomposition for hydrogen production on Ni, Ru and Ni-Ru supported on CeO_2. Int J Hydrogen Energy 2019;44(25):12693–707.
[9] Ganley JC, Thomas FS, Seebauer EG, Masel RI. A priori catalytic activity correlations: the difficult case of hydrogen production from ammonia. Catal Lett 2004;96(3):117–22.
[10] Amano A, Taylor H. The decomposition of ammonia on ruthenium, rhodium and palladium catalysts supported on alumina. J Am Chem Soc 1954;76(16):4201–4.
[11] Choudhary TV, Sivadinarayana C, Goodman DW. Catalytic ammonia decomposition: CO_x–free hydrogen production for fuel cell applications. Catal Lett 2001;72(3):197–201.
[12] Duan X, Qian G, Zhou X, Sui Z, Chen D, Yuan W. Tuning the size and shape of Fe nanoparticles on carbon nanofibers for catalytic ammonia decomposition. Appl Catal, B 2011;101(3):189–96.
[13] Okura K, Miyazaki K, Muroyama H, Matsui T, Eguchi K. Ammonia decomposition over Ni catalysts supported on perovskite-type oxides for the on-site generation of hydrogen. RSC Adv 2018;8(56):32102–10.
[14] Srifa A, Okura K, Okanishi T, Muroyama H, Matsui T, Eguchi K. CO_x–free hydrogen production via ammonia decomposition over molybdenum nitride-based catalysts. Catal Sci Technol 2016;6(20):7495–504.
[15] David WIF, Makepeace JW, Callear SK, Hunter HMA, Taylor JD, Wood TJ, Jones MO. Hydrogen production from ammonia using sodium amide. J Am Chem Soc 2014;136(38):13082–5.
[16] Makepeace JW, Hunter HMA, Wood TJ, Smith RI, Murray CA, David WIF. Ammonia decomposition catalysis using lithium–calcium imide. Faraday Discuss 2016;188:525–44.
[17] Hu X-C, Wang W-W, Jin Z, Wang X, Si R, Jia C-J. Transition metal nanoparticles supported La-promoted MgO as catalysts for hydrogen production via catalytic decomposition of ammonia. J Energy Chem 2019;38:41–9.
[18] Bell TE, Zhan G, Wu K, Zeng HC, Torrente-Murciano L. Modification of ammonia decomposition activity of ruthenium nanoparticles by N-doping of CNT supports. Top Catal 2017;60(15):1251–9.
[19] Gu Y-Q, Jin Z, Zhang H, Xu R-J, Zheng M-J, Guo Y-M, Song Q-S, Jia C-J. Transition metal nanoparticles dispersed in an alumina matrix as active and stable catalysts for CO_x–free hydrogen production from ammonia. J Mater Chem 2015;3(33):17172–80.
[20] Kondo JN, Uchida M, Nakajima K, Daling L, Hara M, Domen K. Synthesis, mesostructure, and photocatalysis of a highly ordered and thermally stable mesoporous Mg and Ta mixed oxide. Chem Mater 2004;16(22):4304–10.
[21] Noda Y, Lee B, Domen K, Kondo JN. Synthesis of crystallized mesoporous tantalum oxide and its photocatalytic activity for overall water splitting under ultraviolet light irradiation. Chem Mater 2008;20(16):5361–7.
[22] Zhu H, Zhao J-C, Liu J, Yang X, Shen Y. General synthesis of a mesoporous composite of metal oxide and silicate nanoparticles from a metal salt and laponite suspension for catalysis. Chem Mater 2006;18(17):3993–4001.
[23] Li Z, Jiaguo Y, Xiujian Z, Bei C, Xiequn Z, Rui G. Research and development of mesoporous nanostructured materials. Rare Met Mater Eng 2004;33(1):5–10.
[24] Laskowski Ł, Laskowska M, Vila N, Schabikowski M, Walcarius A. Mesoporous silica-based materials for electronics-oriented applications. Molecules 2019;24(13):2395.
[25] Julián-López B, Boissière C, Chanéac C, Grosso D, Vasseur S, Miraux S, Duguet E, Sanchez C. Mesoporous maghemite–organosilica microspheres: a promising route towards multifunctional platforms for smart diagnosis and therapy. J Mater Chem 2007;17(16):1563–9.
[26] Chen Y, Chen H, Zhang S, Chen F, Zhang L, Zhang J, Zhu M, Wu H, Guo L, Feng J, Shi J. Multifunctional mesoporous nanoellipsoids for biological bimodal imaging and magnetically targeted delivery of anticancer drugs. Adv Funct Mater 2011;21(2):270–8.
[27] Al-Shehri BM, Khder AERS, Ashour SS, Hamdy MS. A review: the utilization of mesoporous materials in wastewater treatment. Mater Res Express 2019;6(12):122002.
[28] Taguchi A, Schüth F. Ordered mesoporous materials in catalysis. Microporous Mesoporous Mater 2005;77(1):1–45.
[29] Yan H, Xu Y-J, Gu Y-Q, Li H, Wang X, Jin Z, Shi S, Si R, Jia C-J, Yan C-H. Promoted multimetal oxide catalysts for the generation of hydrogen via ammonia decomposition. J Phys Chem C 2016;120(14):7685–96.
[30] Huang C, Li H, Yang J, Wang C, Hu F, Wang X, Lu Z-H, Feng G, Zhang R. $Ce_{0.6}Zr_{0.3}Y_{0.1}O_2$ solid solutions-supported NiCo bimetal nanocatalysts for NH_3 decomposition. Appl Surf Sci 2019;478:708–16.
[31] Lu Y, Fan H, Doke N, Loy DA, Assink RA, LaVan DA, Brinker CJ. Evaporation-induced self-assembly of hybrid bridged silsesquioxane film and particulate mesophases with integral organic functionality. J Am Chem Soc 2000;122(22):5258–61.
[32] Tsung C-K, Fan J, Zheng N, Shi Q, Forman AJ, Wang J, Stucky GD. A general route to diverse mesoporous metal oxide submicrospheres with highly crystalline frameworks. Angew Chem 2008;120(45):8810–4.
[33] Maleki H, Kazemeini M, Larimi AS, Khorasheh F. Transesterification of canola oil and methanol by lithium impregnated CaO–La_2O_3 mixed oxide for biodiesel synthesis. J Ind Eng Chem 2017;47:399–404.
[34] Kruk M, Jaroniec M. Gas adsorption characterization of ordered organic-inorganic nanocomposite materials. Chem Mater 2001;13(10):3169–83.
[35] Hill AK, Torrente-Murciano L. Low temperature H_2 production from ammonia using ruthenium-based catalysts: synergetic effect of promoter and support. Appl Catal, B 2015;172–173:129–35.
[36] Henpraserttae S, Charojrochkul S, Klysubun W, Lawtrakul L, Toochinda P. Reduced temperature ammonia decomposition using Ni/Zr-doped Al_2O_3 catalyst. Catal Lett 2018;148(6):1775–83.
[37] Hayashi F, Toda Y, Kanie Y, Kitano M, Inoue Y, Yokoyama T, Hara M, Hosono H. Ammonia decomposition by ruthenium nanoparticles loaded on inorganic electride C12A7:e^-. Chem Sci 2013;4(8):3124–30.
[38] Huang C, Yu Y, Yang J, Yan Y, Wang D, Hu F, Wang X, Zhang R, Feng G. Ru/La_2O_3 catalyst for ammonia decomposition to hydrogen. Appl Surf Sci 2019;476:928–36.
[39] Hu Z-P, Weng C-C, Yuan G-G, Lv X-W, Yuan Z-Y. Ni nanoparticles supported on mica for efficient decomposition of ammonia to CO_x–free hydrogen. Int J Hydrogen Energy 2018;43(20):9663–76.
[40] Yu Y, Gan Y-M, Huang C, Lu Z-H, Wang X, Zhang R, Feng G. Ni/La_2O_3 and Ni/MgO–La_2O_3 catalysts for the decomposition of NH_3 into hydrogen. Int J Hydrogen Energy 2020;45(33):16528–39.
[41] Zheng W, Zhang J, Ge Q, Xu H, Li W. Effects of CeO_2 addition on Ni/Al_2O_3 catalysts for the reaction of ammonia decomposition to hydrogen. Appl Catal, B 2008;80(1):98–105.

Please cite this article as: Maleki H, Bertola V, Co–Ce–Al–O mesoporous catalysts for hydrogen generation via ammonia decomposition, International Journal of Hydrogen Energy, https://doi.org/10.1016/j.ijhydene.2022.06.021